


# Untying the Growth Index to Relief the $\sigma_8$ Discomfort.

Ziad Sakr<sup>1,2,3</sup> 

<sup>1</sup> Institut für Theoretische Physik, University of Heidelberg, Philosophenweg 16, 69120 Heidelberg, Germany;

<sup>2</sup> IRAP, Université de Toulouse, CNRS, CNES, UPS, Toulouse, France;

<sup>3</sup> Université St Joseph, Faculty of Sciences, Beirut, Lebanon.

**Abstract:** The fluctuation of matter parameter  $\sigma_8$  is by model construction degenerate with the growth index  $\gamma$ . Here we try to study the effect on the cosmological parameters constraints from treating each independently from the other by considering  $\sigma_8$  as a free and not derived parameter along with a free  $\gamma$ , to then try to constrain all by three probes that span from the deep to local redshifts, namely the CMB spectrum, the growth measurements from redshift space distortions  $f\sigma_8$  and the galaxy cluster counts. We also want to assess the impact of this relaxation on the  $\sigma_8$  tension between its value inferred from CMB in comparison to that from cluster counts. We also propose a more sophisticated correction, along with the classical one that takes into account the impact of cosmology on the growth measurements when the parameters are varied in the Monte Carlo process, which is to adjust the growth to keep the observed power spectrum invariant with the background evolution. We found using the classical correction that untying the two parameters does not shift the maximum likelihood on either  $\sigma_8$  or  $\gamma$  but rather allow for larger bounds with respect to when  $\sigma_8$  is a derived parameter, and that when considering CMB+ $f\sigma_8$  or further combining with cluster counts albeit with tighter bounds. More precisely, we obtain  $\sigma_8 = 0.809 \pm 0.043$  and  $\gamma = 0.613 \pm 0.046$  in agreement with Planck constraints for the former and compatible with  $\Lambda$ CDM for the latter but with bounds enough wide to accommodate both values subject of tensions for  $\sigma_8$ . Allowing massive neutrinos does not change much the situation. On the other hand, considering a tier correction yields  $\sigma_8 = 0.734 \pm 0.013$  close to the local values albeit with a growth index  $\gamma = 0.636 \pm 0.022$  a little far from  $\Lambda$ CDM value while allowing a massive neutrinos in this case yielded  $\sigma_8 = 0.756 \pm 0.024$ , still preferring low values but with much looser constraints, with  $\gamma = 0.549 \pm 0.048$  and a slight preference for  $\Sigma m_\nu \sim 0.19$  value. We conclude that untying  $\sigma_8$  and  $\gamma$  helps in relieving the discomfort on the former between CMB and local probes and that careful analyse should be followed when using data obtained in a model dependent way.

**Keywords:** cosmological parameters; large scale structures; growth index; cosmological tensions; matter fluctuation parameter.

## 1. Introduction

The study of the formation of large scale structures (LSS), is one of the strongest tools used to constrain a cosmological model [1] with the essential ingredients necessary to describe them being the matter density, the matter fluctuation calibration parameter,  $\sigma_8$  and the matter growth rate. The latter can be parameterised as a function of the matter density to the power of what we call the growth index  $\gamma$  which value  $\sim 0.55$  was found to well describe the growth in  $\Lambda$ CDM model [2], while deviation from it could signal the need for models beyond the standard cosmological one.

Among the probes that serve to put constraints on these parameters, are the ones we are going to use in this work, such as the cosmic microwave background (CMB) temperatures and polarisations angular power spectrum since it could be related to the growth of the density fluctuations at the recombination epoch [3]; or the measurements of growth in the clustering of galaxies obtained from its effect on the redshifts space distortions (RSD) [4]; or the galaxy cluster counts (CC) or abundance in a given volume [5].

**Citation:** Sakr, Z.; Untying the growth index to relief the  $\sigma_8$  discomfort..

*Preprints* 2023, 1, 0. <https://doi.org/>

**Copyright:** © 2023 by the author. Submitted to *Preprints* for possible open access publication under the terms and conditions of the Creative Commons Attribution (CC BY) license (<https://creativecommons.org/licenses/by/4.0/>).

However, among the three parameters, the CMB measures only directly the matter density, and needs the assumption of a model to derive the  $\sigma_8$  since what is actually measured is rather the amplitude of the power spectrum  $A_s$  that we extrapolate to our time to get the  $\sigma_8$  in a model dependent way. Moreover, the matter density at the recombination epoch is close to unity resulting in little constraining power on the growth index value. While for the other two probes, the growth measurements from the galaxy redshift distortions (RSD) and the cluster counts (CC) measure actually a combination of the three parameters but are not equally sensitive to each of them since the RSD is rather affected by the growth rate of change while the CC is obtained by calibrating a Gaussian halo distribution which average and standard deviation are function of the growth, the  $\sigma_8$  parameter and the matter density at the observed epoch. In general the three are not independent and could be derived from each others if we consider a specific model such as  $\Lambda$ CDM [6]. Moreover, a model is needed for the RSD growth measurements to describe the galaxy bias that relates the underlying matter to the galaxy distribution, while for the cluster counts we need to model the mass observable scaling relation that relates the mass of the halo to that of an observed property of the cluster such as such as its luminosity, richness or temperature.

We can then try to determine the mass observable calibration parameter for the clusters counts from hydrodynamical simulations while for the RSD probe, we often marginalise over the bias if we want to get the growth alone. However, the degeneracy and dependency between  $\Omega_m$ ,  $\sigma_8$  and  $\gamma$  remains and could be alleviated, if we don't want to assume an underlying cosmological model, only if we combine all the three probes as we shall see later. The need to relax the underlying model has become more relevant lately following findings of a persistent tension, varying from 2 to 4  $\sigma$  depending on the datasets used, on the value of  $\sigma_8$  when measured by deep probes such as the CMB, in comparison to that determined from local probes such as the weak lensing measurements or one of our chosen probe, the cluster counts [7–9], but also [10] found a tension on  $\sigma_8$  between RSD and CMB data. Apart from the possibility that it could result from a mis determination of the systematics involved, it could as well be suggesting the need for models beyond LCDM in order to cure this "discomfort".

Consequently, the growth index  $\gamma$  was investigated in [11] and [12] as a way to alleviate this tension, by mean of Bayesian studies using a combination of two of the above probes, CMB and CC, and that in an agnostic approach, where the parameters in relation to the  $\sigma_8$  tension as well as the calibration parameters were left free to vary. When doing so, [12] showed that even if we let the mass observable free, we are still able of putting constraints on  $\gamma$  that, although forbids it from totally solving the tension, however permits to reduce the tension from 4 to 2  $\sigma$  in the case of the cluster sample used. But it was also found that adding neutrinos to the free  $\gamma$  or further relaxing the  $\sigma_8$  value, by considering it as a free parameter and not derived from  $A_s$ , the tension is alleviated albeit with a widening of the constraints, and that even with a fixed  $\gamma$  to the  $\Lambda$ CDM value. Staying with this last restriction on  $\gamma$ , [13] combined the CMB and CC with the growth from the RSD measurements and showed that the combination of the three probes forbid a free  $\sigma_8$  from solving the tension again. However, as mentioned, they did not vary  $\gamma$  but fix it to its  $\Lambda$ CDM value. Moreover, they used the growth measurements as measured assuming  $\Lambda$ CDM while in general when performing MCMC, a correction to account for the effects of the [14] (AP) effect, describing the impact of the change of geometry on the growth of structure with the changing cosmology in the Monte Carlo exploration, is applied. Here we follow the same approach as [13] with the differences that, first we use a larger set of  $f\sigma_8$  measurements that spans over a large range of redshifts. Second, we also let the growth index free to vary (see [15] for a RSD CMB assessment of the tension with modified gravity) in addition to  $\Omega_m$  and  $\sigma_8$  along with the mass observable calibration parameter, and end by further letting free the neutrino mass. Finally, we apply the usual AP correction performed when using growth from RSD measured in different cosmologies. This correction, despite being widely

used, assumes that the adjustment is enough independent of the direction of observation and of its scale dependence. This is not completely true, since the growth measurements are usually extracted from an observed power spectrum that includes such effects on all the scales and observed directions. Already [16] noted that a more sophisticated correction needs to be done, and for that they used a more elaborated one that tried to take into account the direction and the scale above which the power spectrum was measured. However they also assumed small deviations from the fiducial model, sufficient for their purpose since they did not include other probes than the RSD. Here, in addition to the AP correction, we shall also test the impact of a more sophisticated one, relaxing the isotropy assumption along with not supposing small deviations from the fiducial model, and adopting the ansatz that the observed power spectrum used to extract  $f\sigma_8$  is an invariant quantity when the cosmology change, and therefore can be used to determine the new value of the growth rate by adjusting the latter so that to keep the observed power spectrum unchanged as we shall see later.

This paper is organised as follows: in Sect. 2 we present the pipeline and data used in our analysis, as well as the model independent approach followed when combining the different datasets, while we show and discuss our results in Sect. 3 and conclude in Sect. 4.

## 2. Datasets treatment and analysis methods

We perform a MCMC Bayesian study using the CMB  $C_\ell$  of the temperature, polarisation and their cross correlations, from the publicly available datasets of the Planck mission [17] and likelihood [18].

We combine them with the SZ detected clusters sample PSZ2 containing a total of 439 [19] spanning the redshift range from  $z \sim 0.0$  to  $z \sim 1.3$ , where the distribution of clusters function of redshift and signal-to-noise is written as

$$\frac{dN}{dzdq} = \int d\Omega_{\text{mask}} \int dM_{500} \frac{dN}{dzdM_{500}d\Omega} P[q|\bar{q}_m(M_{500}, z, l, b)], \quad (1)$$

with

$$\frac{dN}{dzdM_{500}d\Omega} = \frac{dN}{dVdM_{500}} \frac{dV}{dzd\Omega} \quad (2)$$

Where the halo mass function (HMF) can be written in a simple form [20] :

$$dN/dm = -\frac{\bar{\rho}}{m} \frac{d \ln \nu}{d \ln m} \mathcal{F}(\nu) \quad (3)$$

with  $\nu = \delta_c / \sigma(M, z)$  where  $\sigma(M, z)$ , the variance of the linearly evolved density field smoothed by a spherical top-hat window function  $W$  of comoving radius  $R$  enclosing mass  $M = 4\pi\rho_m R^3/3$ , is

$$\sigma^2(M, z) = \frac{1}{2\pi^2} \int_0^\infty k^2 P_m(k, z) |W_M(k)|^2 dk, \quad (4)$$

The quantity  $P[q|\bar{q}_m(M_{500}, z, l, b)]$  is the distribution of  $q$  given the mean signal-to-noise value,  $\bar{q}_m(M_{500}, z, l, b)$ , predicted by the model for a cluster of mass  $M_{500}$  which we relate to the measured integrated Compton  $y$ -profile  $\bar{Y}_{500}$  using the following scaling relations :

$$E^{-\beta}(z) \left[ \frac{D_A^2(z) \bar{Y}_{500}}{10^{-4} \text{Mpc}^2} \right] = Y_* \left[ \frac{h}{0.7} \right]^{-2+\alpha} \left[ \frac{(1-b) M_{500}}{6 \times 10^{14} M_\odot} \right]^\alpha, \quad (5)$$

All is implemented in our SZ cluster counts module in the framework of the parameter inference Montepython code [21]. When running MCMC chains, we let mainly the normalisation

parameter  $(1 - b)$  for SZ free to vary along with the six CMB cosmological parameters while also leaving  $\alpha$  free since it could be degenerate with the calibration factor.

Since a modified value of the large scale structures growth by mean of that of the growth index  $\gamma$  we define next, enters the HMF through Equ. 4 and changes the cluster number counts, and since this could also happen as well for a certain value of  $\sigma_8$ , defined as the  $z = 0$  variance in the density field at scales of  $8h^{-1} \text{ Mpc}$  and used as a calibration parameter in 4 as we shall also see next, we therefore investigate in this work how the constraints on the cosmological parameters changes when we allow both  $\gamma$  and  $\sigma_8$  to vary, following for  $\gamma$  effect:

$$P_m(k, z, \gamma) = P_m(k, z) \left( \frac{D(z_*)}{D(z)} \frac{D(z, \gamma)}{D(z_*, \gamma)} \right)^2 \quad (6)$$

where  $\gamma$ , the growth index, is the parameter in the phenomenological parameterisation of the growth rate  $f = \Omega_m^\gamma(z)$  and  $f = d \ln D / d \ln a$ ,  $D$  being the growth of perturbations  $\delta(z) = \delta_0 D(z)$ . The growth rate in  $\Lambda$ CDM is well approximated when the growth index is set to  $\sim 0.545$  and takes different values in other modified gravity models [22], while  $\sigma_{8,C}$  used as free calibration parameter would change the power spectrum following:

$$P_m(k, z, \sigma_{8,C}) = P_m(k, z) \left( \frac{\sigma_{8,C}}{\sigma_{8,d}} \right) \quad (7)$$

where C stands for free value used for calibration while  $d$  is for the derived one:

$$\sigma_{8,d} = \frac{1}{2\pi^2} \int dk P_m(k, z=0) |W_{\text{TH}}(kR_8)|^2 k^2, \quad (8)$$

with  $W_{\text{TH}}(x) = 3(\sin x - x \cos x) / x^3$  a top-hat filter in Fourier space.

To break the degeneracies from our model independent approach we use constraints from the growth measurements of the anisotropic clustering of galaxies on the product  $f(z) \sigma_8(z)$  after marginalising over the galaxy bias  $b$ . However, we need to correct from the Alcock-Paczynski (AP) effect or the altering of the distortions in the radial direction by the change of the Hubble parameter  $H(z)$  with cosmology and in the transverse direction by that of the angular diameter distance  $d_A(z)$ . Specifically, we implement the correction as follows [23]: first, we define the ratio of the product of the Hubble parameter  $H(z)$  and the angular diameter distance  $d_A(z)$  for the model at hand to that of the fiducial cosmology,

$$\text{ratio}(z) = \frac{H(z) d_A(z)}{H^{\text{fid}}(z) d_A^{\text{fid}}(z)}, \quad (9)$$

However, as mentioned previously, this method performs a global correction, regardless of the shape of the power spectrum, its calibration, the galaxy matter bias and regardless of a model that could modify the growth apart from those we does it by a propagation of the background. That is why [16] already considered a more sophisticated correction where the  $f\sigma_8$  measurements in the 'new' cosmology could be obtained from the fiducial one following:

$$f\sigma_{8_{\text{new}}} = f\sigma_{8_{\text{fid}}} C \left( \frac{\alpha_{\parallel}}{\alpha_{\perp}^2} \right)_{\text{new}}^{(3/2)} \left( \frac{\sigma_8^{\text{new}}}{\sigma_8^{\text{fid}}} \right)^2, \quad (10)$$

**Table 1.** Compilation of the  $f\sigma_8(z)$  and  $b\sigma_8(z)$  measurements used in this analysis and related references.

$z$	$f\sigma_8(z)$	$\sigma_{f\sigma_8(z)}$	$b\sigma_8(z)$	Ref.
0.15	0.49	0.145	1.445	[24]
0.18	0.392	0.096	0.894	[25]
0.38	0.528	0.072	1.105	[25]
0.25	0.3512	0.0583	1.415	[26]
0.37	0.4602	0.0378	1.509	[26]
0.32	0.394	0.062	1.281	[27]
0.57	0.444	0.038	1.222	[27]
0.22	0.42	0.07	0.664	[28]
0.41	0.45	0.04	0.728	[28]
0.6	0.43	0.04	0.880	[28]
0.78	0.38	0.04	0.973	[28]
0.6	0.55	0.12	0.730	[29]
0.86	0.4	0.11	0.740	[29]
1.4	0.482	0.116	0.814	[30]
0.978	0.379	0.176	0.826	[31]
1.23	0.385	0.099	0.894	[31]
1.526	0.342	0.07	0.953	[31]
1.944	0.364	0.106	1.080	[31]

valid where  $C$  below is considered  $\sim 1$

$$C = \int_{k_1}^{k_2} dk \sqrt{\frac{P_{fid}^m(k)}{P_{new}^m(k')}}. \quad (11)$$

This correction obtained starting from :

$$\beta_{new} = \beta_{fid} C \frac{\mu_{fid}^2}{\mu_{new}^2} \sqrt{\frac{1}{\alpha_{\parallel} \alpha_{\perp}^2}} \quad (12)$$

where  $\beta = f/b$  with  $f$  the growth rate and  $b$  the bias and  $\mu$  the cosine of the angle of sight, needed also to consider that  $\alpha_{\parallel}^2 \approx \alpha_{\perp}^2$  to get,

$$\frac{\mu_{fid}^2}{\mu_{new}^2} \approx \left( \frac{\alpha_{\parallel}}{\alpha_{\perp}} \right)^2, \quad (13)$$

and be able to simplify  $\mu$  from the equation. Finally, it needs also to consider that the bias measured is proportional to the  $\sigma_8$  value.

Here we keep the assumption on the bias but relax the other assumptions and try to correct the growth measurements by mean of the ratio of the observed power spectrum in the fiducial cosmology to the one in the new cosmology varied with each step of the Monte Carlo chain method following the idea that the observed spectrum should remain invariant since it is an observation. This method allow us also to incorporate the bias since it is a part of the observed power spectrum while in other studies the  $f\sigma_8$  values are provided marginalising over it. For that we recompiled the set of measurements choosing from the different surveys the couple of  $f$  and  $b$  that they provided which could be different from the  $f$  value usually obtained when marginalising over the bias. We are by then trying to benefit from the effects of the cosmological parameters variation on the integrated full shape of the power spectrum with

the hope that this constrain will serve to further reduce the degeneracy coming from the extra degrees of freedom considered in our model independent approach.

In practice, starting from the 'fiducial' measurements we consider that the observed power spectrum should stay the same while the model parameters changes we are then able of equating with the new observed power spectrum where the (') symbol was used to denote it.

$$C_{fid} = \int_{k_1}^{k_2} \int_{\mu_1}^{\mu_2} \left( b(z)\sigma_8(z) + f(z)\sigma_8(z) \mu^2 \right)^2 \frac{P_m(k, z)}{\sigma_8^2(z)} d\mu dk \quad (14)$$

$$\int_{k'_1}^{k'_2} \int_{\mu'_1}^{\mu'_2} \left( b'(z)\sigma'_8(z) + f'(z)\sigma'_8(z) \mu'^2 \right)^2 \frac{P'_m(k', z)}{\sigma'^2_8(z)} d\mu dk = C_{fid} \quad (15)$$

We solve for  $f'\sigma'_8$  as function of  $C_{fid}$  which is a known value, and  $P'_m/\sigma'_8$  which is known in the new cosmology regardless of the value of  $\gamma$ , and  $b'\sigma'_8$  also known assuming the bias is proportional to the modified  $\sigma_8$  in the new set of parameters.

### 3. Results

We start by showing in Fig. 1 the impact on the MCMC inferred constraints from considering both  $\gamma$  and  $\sigma_8$  as a free parameter in comparison to those obtained when the growth index is free but  $\sigma_8$  is derived using Equ. 8. When adopting the first prescription,  $\sigma_{8,f}$  becomes effectively the one driving the observable theoretical prediction, that is why we show both, the derived and free one on the same plot. We also show the results from combining CMB data and growth measurements data in comparison to further adding cluster counts constraints. Here we use growth measurements compiled by [32] and follow the global correction of Equ. 9 to account for the AP effects. As expected, the constraints are tighter when less free parameter are considered. We also observe that when  $\gamma$  is the only free parameter, the constraints from CMB +  $f\sigma_8$  do not show substantial change with respect to that when we add cluster counts because the growth is already fixed by the CMB and  $f\sigma_8$  combination while leaving  $\gamma$  and  $\sigma_8$  free add a degeneracy that needs the contribution of the cluster constraints to be broken, which results in tighter contours with respect to the case of using CMB +  $f\sigma_8$  only. While the derived  $\sigma_8$  value is compatible with that usually inferred from CMB, considering  $\sigma_8$  as a free parameter widens the constraints, allowing a range that covers values for  $\sigma_8$  that are usually obtained from either deep or local probes. It permits by then to relief the  $\sigma_8$  discomfort essentially because it also allows larger bounds on  $\gamma$  though still staying compatible with 0.55 the  $\Lambda$ CDM value while in the case where only  $\gamma$  is left free, the latter is forbidden from exploring values that reconcile CMB and cluster counts measurements, and that remains even if we additionally combine with cluster counts, albeit from a tightening in the constraints in this case due to the fact that even if  $\sigma_8$  is not fixed by CMB anymore, the combination of  $f\sigma_8$ +CC constrain and break the degeneracy on the growth and the normalisation of the fluctuation of parameter on local redshifts all together while the presence of CMB is still needed to constrain the matter density.

Before we discuss the impact of the correction that relies on rescaling the observed linear power spectrum entering the growth measurement for the AP effect rather than limiting to the global correction, we want to check whether the new compilation needed to perform the new correction is compatible with the standard compilation. For that we show in Fig. 2 a comparison between the constraints inferred from the two compilations using the same AP correction. The two constraints are compatible despite the difference in some of the datasets that were omitted or added to the SN compilation and despite the fact that some values for  $f\sigma_8$  differs even for a common datasets since we considered the  $f\sigma_8$  obtained without marginalising

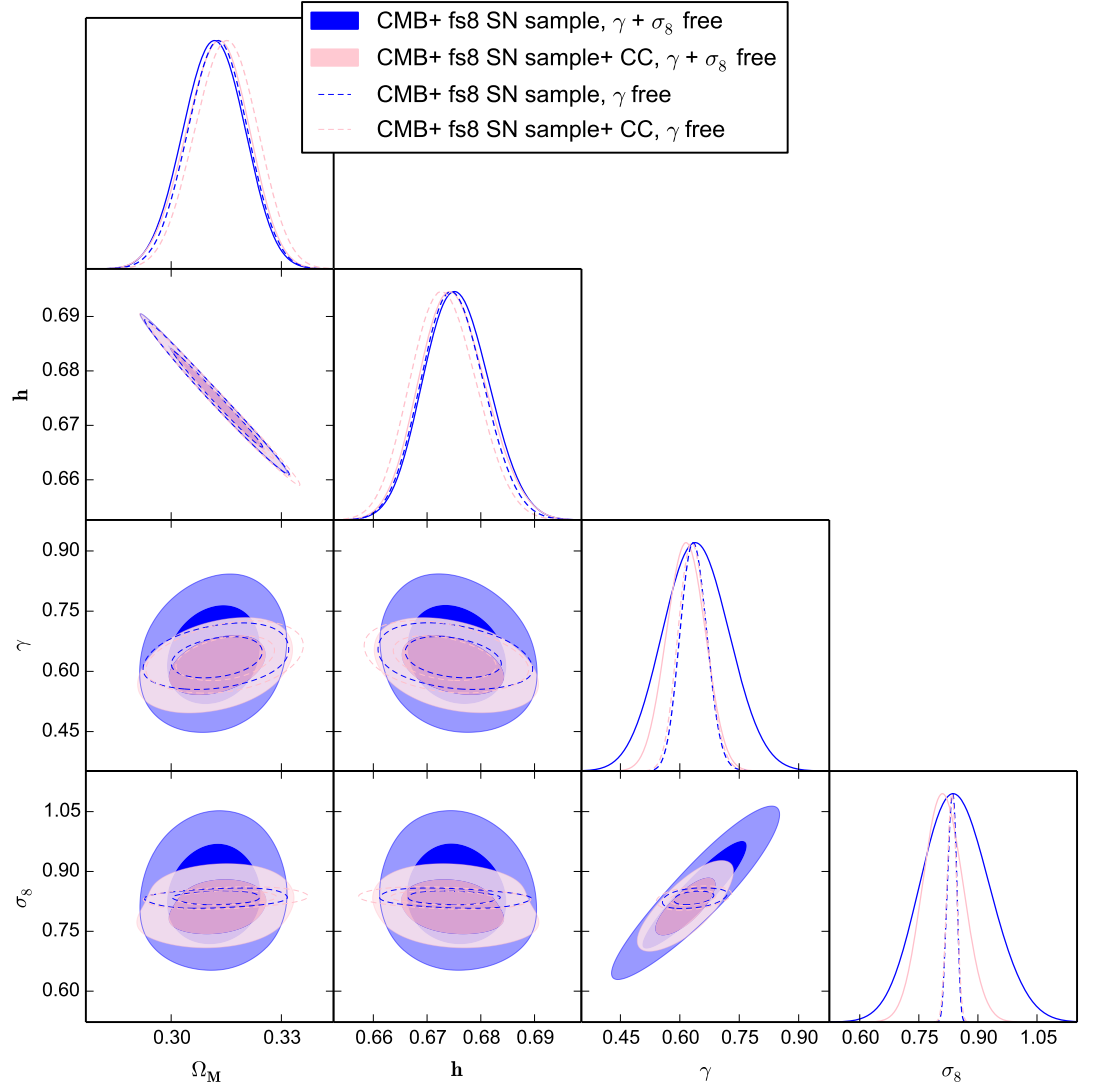


**Figure 1.** 68% and 95% confidence contours for  $\Omega_m$ ,  $h$ ,  $\gamma$  and a derived  $\sigma_8$ , all inferred from a combination of CMB  $C_\ell^{TT,TE,EE}$  Planck 2018,  $f\sigma_8$  measurements from [32] and SZ detected cluster counts (dashed lines) in comparison to those on  $\Omega_m$ ,  $h$  and  $\gamma$  with  $\sigma_8$  as a free parameter using the same probes.



over the bias. Here we only show the sufficient extreme case of letting both  $\gamma$  and  $\sigma_8$  free. We also notice that the agreement is bigger when we add cluster counts since as expected the latter further limit the shift or widening of the contours induced from choosing different values of  $f\sigma_8$  for the two compilation of growth measurements sets.

Having established the compatibility between the two combination of datasets we now show in Fig. 3 the impact in the  $\gamma + \sigma_8$  free case when considering the AP correction on the scale of the power spectrum in comparison to the global one. We observe that the correction introduced makes the model more stiff and strongly tighten the contours especially on our two parameters  $\gamma$  and  $\sigma_8$ . The former is then constrained tightly around  $\sim 0.66$  without forbidding the latter from showing preferences for values compatible with cluster counts. We also notice that the improvement from adding Cluster count is small here since the correction boosts the constraints from  $f\sigma_8$  while cluster counts are not affected by it.

Finally the massive neutrinos have been proposed to solve the  $\sigma_8$  tension due to the fact that they free stream from the halo gravitational potentials lowering by then the power spectrum. However, [11] has shown that they are not able, especially when CMB+cluster counts are further combined with BAO, to fix the tension on  $\sigma_8$  even if we further allow  $\gamma$  to vary. Here we also consider a case with free massive neutrinos in our two schemes with  $f\sigma_8$  data but without adding BAO constraints. However, we also allow, as above,  $\sigma_8$  and  $\gamma$  free with massive neutrinos using first the usual AP correction, where the neutrinos impact enters from its effects on the background evolution that translate into those on  $d_A$  and  $H(z)$ . We observe in Fig. 4 that introducing neutrinos have an impact this time on  $h$  and  $\Omega_M$  parameters skewing both to large and smaller values respectively with however each effect compensating the other, also seen from the observed correlation between  $h$  and  $\Omega_M$ , resulting in a small effect on  $\gamma$  and even smaller on  $\sigma_8$  suggesting that even with more degrees of freedom, still neutrinos does not have a substantial impact on solving the tension. But if we consider now our more tiered correction with the same free parameters, we observe in Fig. 5 that allowing massive neutrinos relax the stiffness of the correction we previously considered and allow for larger bounds on all parameters still leaving the constraints on  $\sigma_8$  compatible with cluster counts, as it was the case with massless neutrinos, while keeping  $\gamma$  within  $\Lambda$ CDM value at the expense of showing a small preference for a non vanishing value for its mass thus also calling for attention to be taken when assessing the bounds on neutrinos from growth or structure formation observations.

#### 4. Conclusions

In this work, we performed a Bayesian study in order to obtain constraints on the cosmological parameters, in particular the matter fluctuation parameter  $\sigma_8$ , when additionally varying the growth index  $\gamma$ , using three probes, the CMB angular power spectrum, RSD from galaxy clustering and galaxy clusters abundance. Usually, due to the interdependency between the effects of the two parameters, two of the aforementioned three probes are sufficient to constrain them. However, here we further tried a model independent approach, by introducing two additional degree of freedom by mean of a parameter that rescales the value of  $\sigma_8$  as well as by letting free the mass observable calibration parameter for the cluster counts probe. This is further motivated by the existence of a small discrepancy between the value of  $\sigma_8$  on that obtained from cluster counts with respect to that inferred from CMB data that could as well be degenerate with the growth of structure and by then  $\gamma$ . Since it was already found in [12] that the combination of CMB and SZ detected cluster counts in the presence of a free growth index  $\gamma$  is barely able of alleviating the discrepancy even if we also relax the mass observable calibration parameter, due to the tomographic constraints put on the growth at different redshifts, we are expecting that the further combination with  $f\sigma_8$  data would further constrain  $\gamma$  from fixing the



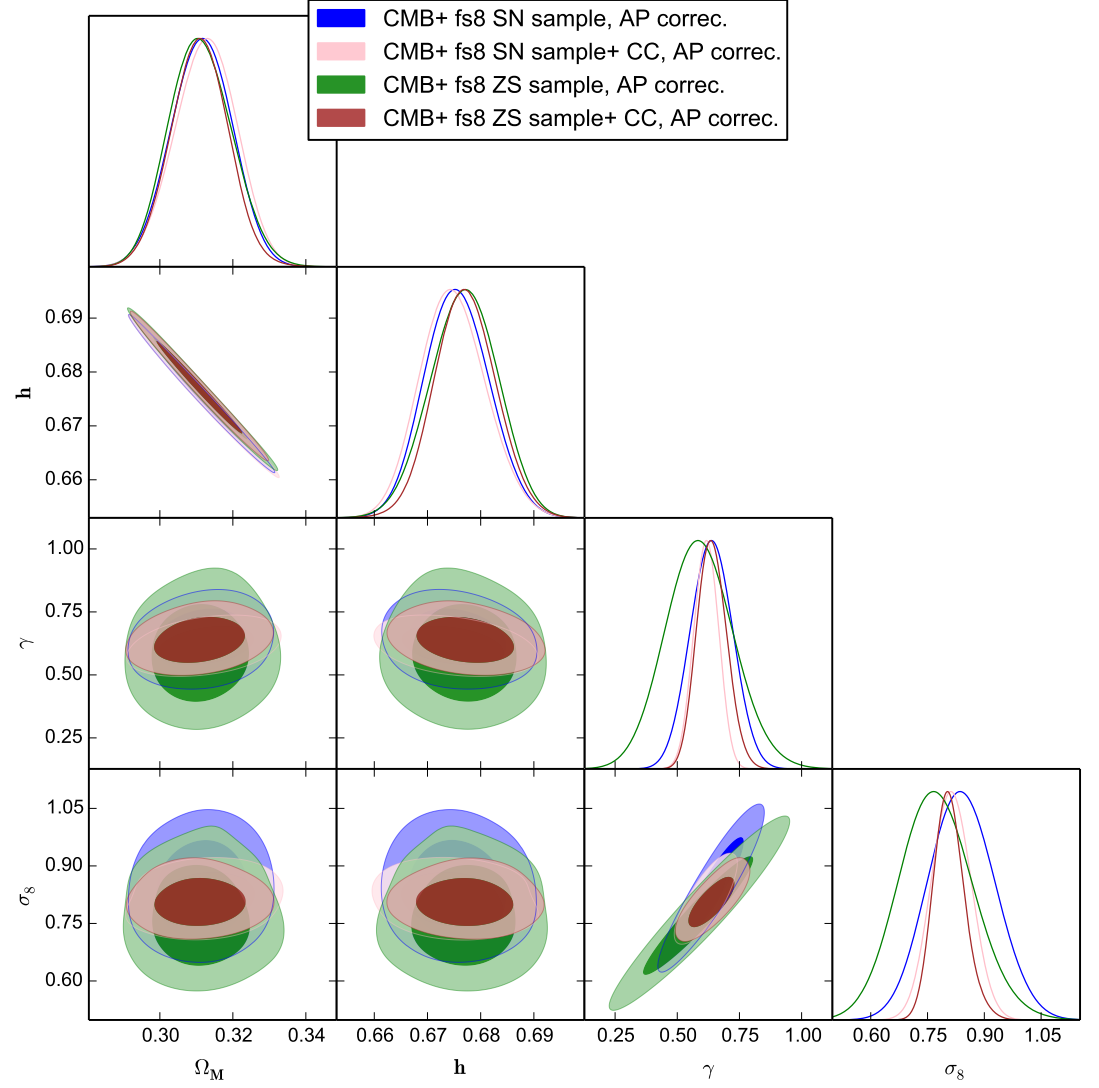


**Figure 2.** 68% and 95% confidence contours for  $\Omega_m$ ,  $h$ ,  $\gamma$  and a free  $\sigma_8$ , all inferred from a combination of CMB  $C_\ell^{TT,TE,EE}$  Planck 2018, SZ detected cluster counts and  $f\sigma_8$  measurements from [32] corrected by rescaling the final observation for the AP effect, in comparison to those inferred using the same probes but using instead  $f\sigma_8$  measurements from Table 1 using the same correction method.

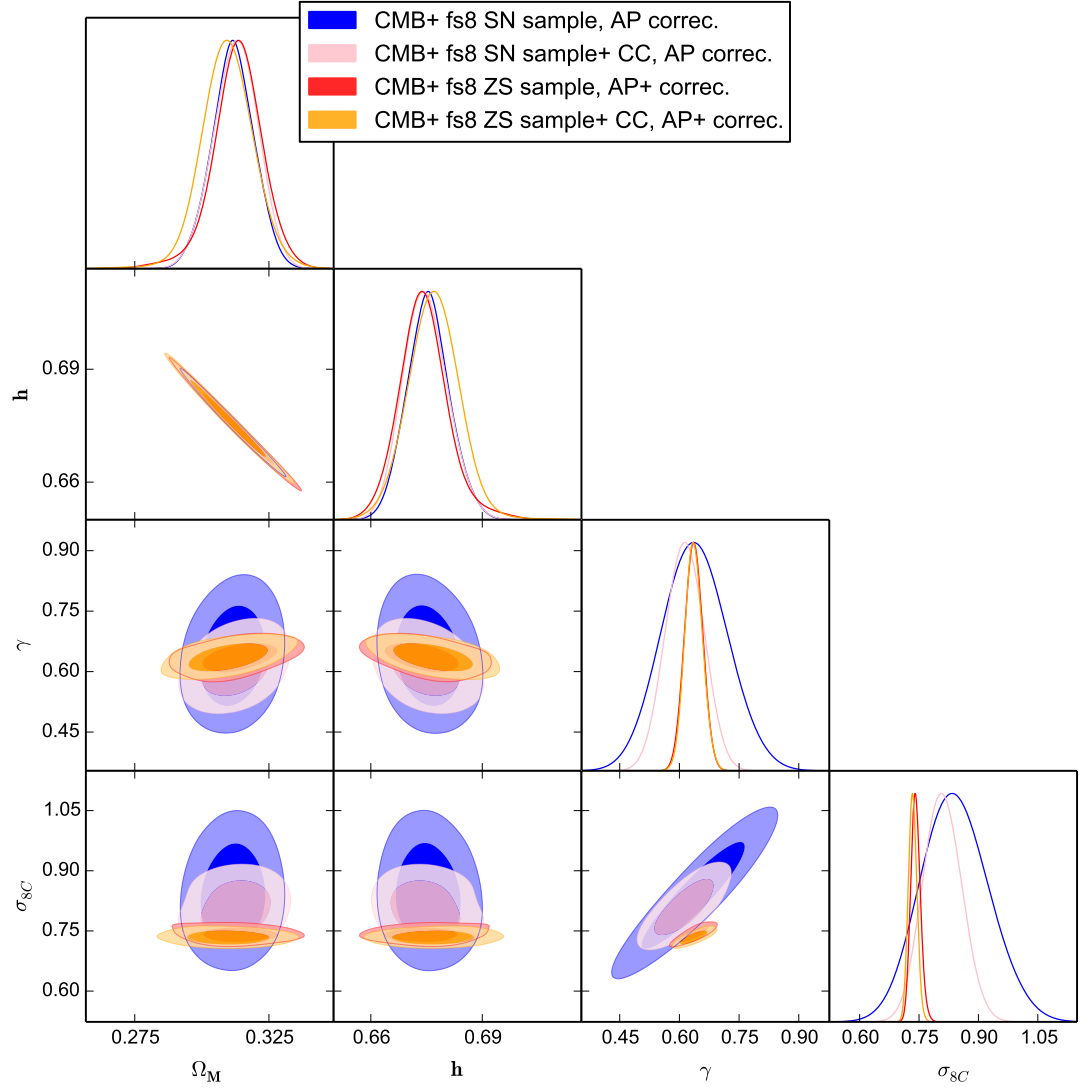


**Figure 3.** 68% and 95% confidence contours for  $\Omega_m$ ,  $h$ ,  $\gamma$  and a free  $\sigma_8$ , all inferred from a combination of CMB  $C_\ell^{TT,TE,EE}$  Planck 2018, SZ detected cluster counts and  $f\sigma_8$  measurements from [32] corrected by rescaling the final observation for the AP effect, in comparison to those inferred using the same probes but using instead  $f\sigma_8$  measurements from Table 1 corrected by rescaling the observed linear power spectrum entering the growth measurement for the AP effect.

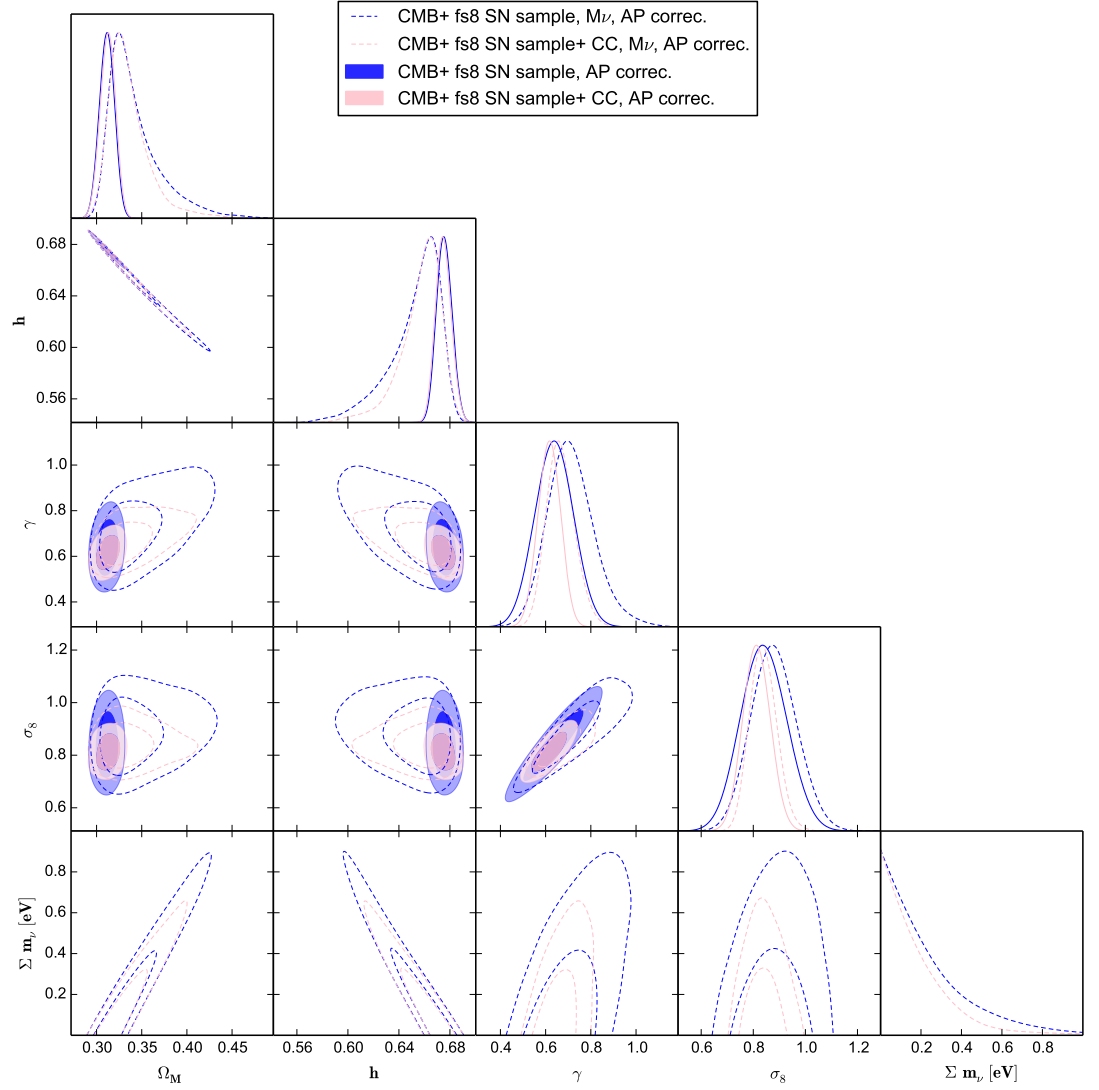


**Figure 4.** 68% and 95% confidence contours for  $\Omega_m$ ,  $h$ ,  $\gamma$  and a free  $\sigma_8$ , all inferred from a combination of CMB  $C_\ell^{TT,TE,EE}$  Planck 2018, SZ detected cluster counts and  $f\sigma_8$  measurements from [32] corrected by rescaling the final observation for the AP effect for the case of massless neutrino in comparison to when considering massive neutrinos.

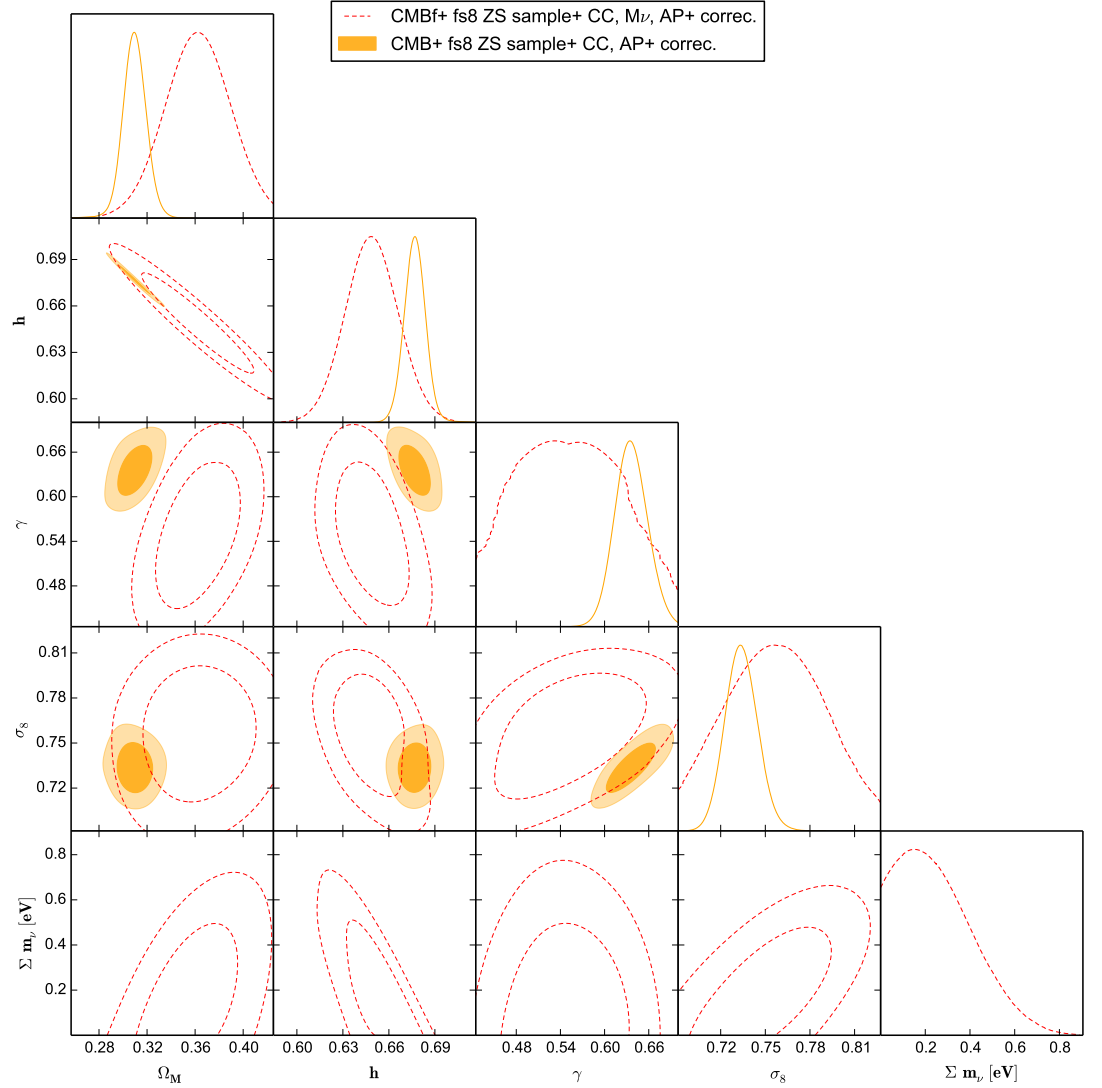


**Figure 5.** 68% and 95% confidence contours for  $\Omega_m$ ,  $h$ ,  $\gamma$  and a free  $\sigma_8$  with massive neutrinos, all inferred from a combination of CMB  $C_\ell^{TT,TE,EE}$  Planck 2018, SZ detected cluster counts and  $f\sigma_8$  measurements from [32] corrected by rescaling the final observation for the AP effect in comparison to  $f\sigma_8$  measurements from Table 1 corrected by corrected by rescaling the linear power spectrum entering the growth measurement for the AP effect.

discrepancy. However this is obtained with a model dependency relating the calibration of the amplitude of the CMB power spectrum to that of nowadays value of  $\sigma_8$  through the growth rate parameterised by  $\gamma$  while here, by further considering  $\sigma_8$  a free and not derived parameter, we expect to further relax the previous constraints in the hope of reducing or fixing the tension.

We found that allowing a free  $\sigma_8$  does indeed widen the constraints on the latter if the  $f\sigma_8$  measurements are combined with CMB and to a lesser but still substantial degree if we further add cluster counts data, and that using the common global AP geometrical correction usually performed to the growth measurements to account for every new set of parameters explored by the MCMC inference method. And we found that the growth index bounds are also still in agreement with the equivalent  $\Lambda$ CDM values. However, when we tried a more sophisticated correction based on geometrically rescaling the power spectrum entering the growth measurements as well as the bias relating the observed galaxy correlation with respect to the matter distribution, we found that the constraints were tightened again but the discrepancy was still fixed through a shift towards the local values with a growth index in slight disagreement with its  $\Lambda$ CDM value. Allowing further free massive neutrinos, an ingredient often advocated as a solution to fix the discrepancy, though not alone as shown by [11], only slightly reduces the discrepancy and that by relaxing the constraints in all cases including the most tightening ones when the three probes CMB,  $f\sigma_8$  and CC are combined, and that in the case of the classical AP global correction. However, when using the more tired correction, we observe that neutrino relatively relaxes more the constraints with respect to the case with massless neutrinos, with values of  $\sigma_8$  still in agreement with local ones and  $\gamma$  with its  $\Lambda$ CDM fiducial, while neutrinos mass are now showing a small preference for a non vanishing value.

We conclude that untying the growth index from  $\sigma_8$  helps in reducing the tension but that special care should be followed in the treatment and analysis of the data in order to relax its model dependency so that to better understand the discrepancy's significance and its impact on the viability of the  $\Lambda$ CDM model.

**Acknowledgments:** Z.S. acknowledges funding from DFG project 456622116 and support from the IRAP Toulouse and IN2P3 Lyon computing centres.

## References

1. Jones, B.J.T. The large scale structure of the universe. In *Observational and Physical Cosmology*; Sanchez, F.; Collados, M.; Rebollo, R., Eds.; 1992; p. 171.
2. Peebles, P.J.E. *The large-scale structure of the universe*; 1980.
3. Hu, W.; Sugiyama, N.; Silk, J. The Physics of microwave background anisotropies. *Nature* **1997**, *386*, 37–43, [[astro-ph/9604166](#)]. <https://doi.org/10.1038/386037a0>.
4. Hamilton, A.J.S. Redshift Distortions and Omega in IRAS Surveys. In Proceedings of the 30th Rencontres de Moriond: Euroconferences: Clustering in the Universe, 1995, pp. 143–156, [[astro-ph/9507022](#)].
5. Kravtsov, A.V.; Borgani, S. Formation of Galaxy Clusters. *araa* **2012**, *50*, 353–409, [[1205.5556](#)]. <https://doi.org/10.1146/annurev-astro-081811-125502>.
6. White, S.D.M.; Efstathiou, G.; Frenk, C.S. The amplitude of mass fluctuations in the universe. *mnras* **1993**, *262*, 1023–1028. <https://doi.org/10.1093/mnras/262.4.1023>.
7. Planck Collaboration.; Ade, P.A.R.; Aghanim, N.; Armitage-Caplan, C.; Arnaud, M.; Ashdown, M.; Atrio-Barandela, F.; Aumont, J.; Aussel, H.; Baccigalupi, C.; et al. Planck 2013 results. XXIX. The Planck catalogue of Sunyaev-Zeldovich sources. *aap* **2014**, *571*, A29, [[1303.5089](#)]. <https://doi.org/10.1051/0004-6361/201321523>.
8. Hildebrandt, H.; Köhlinger, F.; van den Busch, J.L.; Joachimi, B.; Heymans, C.; Kannawadi, A.; Wright, A.H.; Asgari, M.; Blake, C.; Hoekstra, H.; et al. KiDS+VIKING-450: Cosmic shear tomography with optical and infrared data. *aap* **2020**, *633*, A69, [[arXiv:astro-ph.CO/1812.06076](#)]. <https://doi.org/10.1051/0004-6361/201834878>.
9. Amon, A.; et al. Dark Energy Survey Year 3 results: Cosmology from cosmic shear and robustness to data calibration. *Phys. Rev. D* **2022**, *105*, 023514, [[arXiv:astro-ph.CO/2105.13543](#)]. <https://doi.org/10.1103/PhysRevD.105.023514>.

10. Benisty, D. Quantifying the  $S_8$  tension with the Redshift Space Distortion data set. *Phys. Dark Univ.* **2021**, *31*, 100766, [arXiv:astro-ph.CO/2005.03751]. <https://doi.org/10.1016/j.dark.2020.100766>.
11. Sakr, Z.; Ilić, S.; Blanchard, A.; Bittar, J.; Farah, W. Cluster counts: Calibration issue or new physics? *Astron. Astrophys.* **2018**, *620*, A78, [arXiv:astro-ph.CO/1803.11170]. <https://doi.org/10.1051/0004-6361/201833151>.
12. Ilić, S.; Sakr, Z.; Blanchard, A. Cluster counts. II. Tensions, massive neutrinos, and modified gravity. *Astron. Astrophys.* **2019**, *631*, A96, [arXiv:astro-ph.CO/1908.00163]. <https://doi.org/10.1051/0004-6361/201936423>.
13. Blanchard, A.; Héloret, J.Y.; Ilić, S.; Lamine, B.; Tutusaus, I.  $\Lambda$ CDM is alive and well **2022**. [arXiv:astro-ph.CO/2205.05017].
14. Alcock, C.; Paczynski, B. An evolution free test for non-zero cosmological constant. *Nature* **1979**, *281*, 358–359. <https://doi.org/10.1038/281358a0>.
15. Kazantzidis, L.; Perivolaropoulos, L. Evolution of the  $f\sigma_8$  tension with the Planck15/ $\Lambda$ CDM determination and implications for modified gravity theories. *Phys. Rev. D* **2018**, *97*, 103503, [arXiv:astro-ph.CO/1803.01337]. <https://doi.org/10.1103/PhysRevD.97.103503>.
16. Alam, S.; Ho, S.; Silvestri, A. Testing deviations from  $\Lambda$ CDM with growth rate measurements from six large-scale structure surveys at  $z = 0.06$ – $1$ . *mnras* **2016**, *456*, 3743–3756, [arXiv:astro-ph.CO/1509.05034]. <https://doi.org/10.1093/mnras/stv2935>.
17. Aghanim, N.; et al. Planck 2018 results. VI. Cosmological parameters. *Astron. Astrophys.* **2020**, *641*, A6, [arXiv:astro-ph.CO/1807.06209]. <https://doi.org/10.1051/0004-6361/201833910>.
18. Aghanim, N.; et al. Planck 2018 results. V. CMB power spectra and likelihoods. *Astron. Astrophys.* **2020**, *641*, A5, [arXiv:astro-ph.CO/1907.12875]. <https://doi.org/10.1051/0004-6361/201936386>.
19. Planck Collaboration.; Ade, P.A.R.; Aghanim, N.; Arnaud, M.; Ashdown, M.; Aumont, J.; Baccigalupi, C.; Banday, A.J.; Barreiro, R.B.; Barrera, R.; et al. Planck 2015 results. XXVII. The second Planck catalogue of Sunyaev-Zeldovich sources. *aap* **2016**, *594*, A27, [arXiv:astro-ph.CO/1502.01598]. <https://doi.org/10.1051/0004-6361/201525823>.
20. Blanchard, A.; Valls-Gabaud, D.; Mamon, G.A. The origin of the galaxy luminosity function and the thermal evolution of the intergalactic medium. *aap* **1992**, *264*, 365–378.
21. Brinckmann, T.; Lesgourgues, J. MontePython 3: boosted MCMC sampler and other features. *Phys. Dark Univ.* **2019**, *24*, 100260, [arXiv:astro-ph.CO/1804.07261]. <https://doi.org/10.1016/j.dark.2018.100260>.
22. Linder, E.V.; Cahn, R.N. Parameterized Beyond-Einstein Growth. *Astropart. Phys.* **2007**, *28*, 481–488, [astro-ph/0701317]. <https://doi.org/10.1016/j.astropartphys.2007.09.003>.
23. Arjona, R.; García-Bellido, J.; Nesseris, S. Cosmological constraints on nonadiabatic dark energy perturbations. *Phys. Rev. D* **2020**, *102*, 103526, [arXiv:astro-ph.CO/2006.01762]. <https://doi.org/10.1103/PhysRevD.102.103526>.
24. Howlett, C.; Ross, A.; Samushia, L.; Percival, W.; Manera, M. The clustering of the SDSS main galaxy sample – II. Mock galaxy catalogues and a measurement of the growth of structure from redshift space distortions at  $z = 0.15$ . *Mon. Not. Roy. Astron. Soc.* **2015**, *449*, 848–866, [arXiv:astro-ph.CO/1409.3238]. <https://doi.org/10.1093/mnras/stu2693>.
25. Blake, C.; et al. Galaxy And Mass Assembly (GAMA): improved cosmic growth measurements using multiple tracers of large-scale structure. *Mon. Not. Roy. Astron. Soc.* **2013**, *436*, 3089, [arXiv:astro-ph.CO/1309.5556]. <https://doi.org/10.1093/mnras/stt1791>.
26. Samushia, L.; Percival, W.J.; Raccañelli, A. Interpreting large-scale redshift-space distortion measurements. *Mon. Not. Roy. Astron. Soc.* **2012**, *420*, 2102–2119, [arXiv:astro-ph.CO/1102.1014]. <https://doi.org/10.1111/j.1365-2966.2011.20169.x>.
27. Gil-Marín, H.; et al. The clustering of galaxies in the SDSS-III Baryon Oscillation Spectroscopic Survey: RSD measurement from the LOS-dependent power spectrum of DR12 BOSS galaxies. *Mon. Not. Roy. Astron. Soc.* **2016**, *460*, 4188–4209, [arXiv:astro-ph.CO/1509.06386]. <https://doi.org/10.1093/mnras/stw1096>.
28. Blake, C.; et al. The WiggleZ Dark Energy Survey: the growth rate of cosmic structure since redshift  $z=0.9$ . *Mon. Not. Roy. Astron. Soc.* **2011**, *415*, 2876, [arXiv:astro-ph.CO/1104.2948]. <https://doi.org/10.1111/j.1365-2966.2011.18903.x>.
29. Pezzotta, A.; et al. The VIMOS Public Extragalactic Redshift Survey (VIPERS): The growth of structure at  $0.5 < z < 1.2$  from redshift-space distortions in the clustering of the PDR-2 final sample. *Astron. Astrophys.* **2017**, *604*, A33, [arXiv:astro-ph.CO/1612.05645]. <https://doi.org/10.1051/0004-6361/201630295>.
30. Okumura, T.; et al. The Subaru FMOS galaxy redshift survey (FastSound). IV. New constraint on gravity theory from redshift space distortions at  $z \sim 1.4$ . *Publ. Astron. Soc. Jap.* **2016**, *68*, 38, [arXiv:astro-ph.CO/1511.08083]. <https://doi.org/10.1093/pasj/psw029>.
31. Zhao, G.B.; et al. The clustering of the SDSS-IV extended Baryon Oscillation Spectroscopic Survey DR14 quasar sample: a tomographic measurement of cosmic structure growth and expansion rate based on optimal redshift weights. *Mon. Not. Roy. Astron. Soc.* **2019**, *482*, 3497–3513, [arXiv:astro-ph.CO/1801.03043]. <https://doi.org/10.1093/mnras/sty2845>.
32. Sagredo, B.; Nesseris, S.; Sapone, D. Internal robustness of growth rate data. *prd* **2018**, *98*, 083543, [arXiv:astro-ph.CO/1806.10822]. <https://doi.org/10.1103/PhysRevD.98.083543>.